

Influence of Covalency upon Rare-Earth Ligand Field Splittings

J. D. AXE AND GERALD BURNS

IBM Watson Research Center, Yorktown Heights, New York

(Received 25 April 1966)

Experimental results for the shift with uniaxial stress of the (${}^2F_{5/2}, \Gamma_7$) \rightarrow (${}^2F_{7/2}, \Gamma_7$) laser transition in $\text{Tm}^{2+}:\text{CaF}_2$ and $\text{Tm}^{2+}:\text{SrF}_2$ are presented. The results, $1.75 \text{ cm}^{-1}(\text{dyn}/\text{cm}^2)^{-1}$ and $1.78 \text{ cm}^{-1}(\text{dyn}/\text{cm}^2)^{-1}$, are used to calculate the radial dependence of the cubic ligand field splitting. The resulting dependence is somewhat larger than that predicted by the familiar electrostatic model for the splitting. Partially to determine its influence on the above result, we have considered the effect of covalency by means of a semiempirical molecular-orbital model. The overlap of the $4f$ orbitals with the neighboring fluoride ions was calculated using Hartree-Fock wave functions and known internuclear distances. The off-diagonal elements of the interaction Hamiltonian were obtained from the Wolfsberg-Helmholz approximation $H_{ij} = 2S_{ij}(H_{ii} + H_{jj})/2$. A range of reasonable values for the diagonal elements were obtained by analogy with those necessary to explain iron-series splittings. The largest group overlap of the $4f$ wave function with F^{1-} ligands was found to be 3.6% and leads to a sizable (our best estimate in CaF_2 is 50%) covalent contribution to the ligand field splitting. We have also investigated some of the consequences of a covalent contribution of this magnitude. The radial dependence of the covalent part of the energy is greater than for the electrostatic part. The resulting radial dependence is thus in better agreement with experiment. Transferred hyperfine effects are calculated and compared to experiment, but the extent of the agreement is hard to ascertain because of uncertainty of the sign of the experimental quantity and polarization effects. The calculated orbital reduction factor for $\text{Tm}^{2+}:\text{CaF}_2$ is found to be much smaller than is observed. We have also calculated the expected variation of the (rare earth) $^{3+}$ - F^{1-} overlap as a function of atomic number.

INTRODUCTION

THE theory of the low-lying electronic levels of transition-metal and rare-earth ions in solids was initially advanced upon the hypothesis that the major forces acting upon these magnetic electrons were of a classical electrostatic nature. The theory has had many successes as applied to both systems. However, a closer look at some of the data of the transition-metal ions (transferred hyperfine structure, orbital moment reduction, etc.) has led to the realization that the crystal-field splittings arise predominantly from covalent effects. On the other hand, the $4f$ electrons in rare-earth (R.E.) ions are much less exposed for bonding purposes than are the $3d$ electrons. Thus, it was usually supposed that longer range electrostatic forces predominate the (considerably smaller) observed $4f$ splittings. However, detailed calculations based upon an electrostatic model have been attempted and have met with indifferent success.¹⁻³ While it is possible that explicit consideration of shielding^{2,4-6} and polarization⁷ effects will reduce the discrepancy, such covalent effects as transferred ligand hfs have been observed,^{8,9} and Jorgensen *et al.*¹⁰ argue that rare-earth crystal-field

splitting might be better understood as a weak σ -anti-bonding effect.

In studying crystal-field effects, comparatively little attention has been given to changes induced by uniaxial or hydrostatic pressure. Uniaxial stresses have been used to establish the point symmetry of the rare-earth defects¹¹ and to determine if the transition involves a $5d$ level.^{12,13} We felt that strain experiments on $4f$ to $4f$ transitions in rare-earth ions at high symmetry sites could be of importance since the strain is equivalent to an additional crystal field of variable symmetry and strength. The alkaline-earth fluoride-divalent thulium combination was chosen as one possessing the following advantages. The spectrum of Tm^{2+} , a single "hole" in an otherwise completed $4f$ shell, is relatively simple and well understood. Previous optical¹⁴ and spin-resonance studies^{9,15} have reported much subsidiary information. One of the fluorescent transitions is sharp and intense. Symmetry imposes a very simple form for the strain interaction. Finally by substituting SrF_2 for CaF_2 as a host matrix, an additional degree of freedom can be introduced and investigated. The CaF_2 result has been reported previously¹⁶ and the results in SrF_2 here. In both cases the crystal field appears to depend on a larger negative power of the internuclear distance than predicted by the ionic model providing the microscopic stress-strain relation is taken to be identical to that

¹ C. A. Hutchison and E. Y. Wong, *J. Chem. Phys.* **29**, 754 (1958); and E. Y. Wong and I. Richman, *ibid.* **36**, 1889 (1962).

² G. Burns, *Phys. Rev.* **128**, 2121 (1962).

³ M. T. Hutchings and D. K. Ray, *Proc. Roy. Soc. (London)* **81**, 633 (1963).

⁴ C. J. Lenander and E. Y. Wong, *J. Chem. Phys.* **38**, 2750 (1963).

⁵ D. K. Ray, *Proc. Phys. Soc. (London)* **82**, 47 (1963).

⁶ R. E. Watson and A. J. Freeman, *Phys. Rev.* **133**, A1571 (1964).

⁷ G. Burns, *J. Chem. Phys.* **42**, 377 (1965).

⁸ J. M. Baker and J. P. Hurrell, *Proc. Phys. Soc. (London)* **82**, 742 (1963).

⁹ R. G. Bessent and W. Hayes, *Proc. Roy. Soc. (London)* **A285**, 430 (1964).

¹⁰ C. K. Jorgensen, R. Pappalardo, and H. H. Smidtke, *J. Chem. Phys.* **39**, 1422 (1963).

¹¹ A. A. Kaplanski, *Opt. Spectry. (USSR)* **7**, 406 (1959).

¹² W. A. Runcimann and C. V. Stager, *J. Chem. Phys.* **38**, 279 (1963).

¹³ For a general review of high pressure hydrostatic strain effects see H. G. Drickamer, in *Solid State Physics*, edited by F. Seitz and D. Turnbull (Academic Press Inc., New York, 1965), Vol. 17.

¹⁴ Z. J. Kiss, *Phys. Rev.* **127**, 718 (1962).

¹⁵ W. Hayes and J. W. Twidell, *J. Chem. Phys.* **35**, 152 (1961).

¹⁶ G. Burns and J. D. Axe, *Phys. Letters* **19**, 98 (1965).

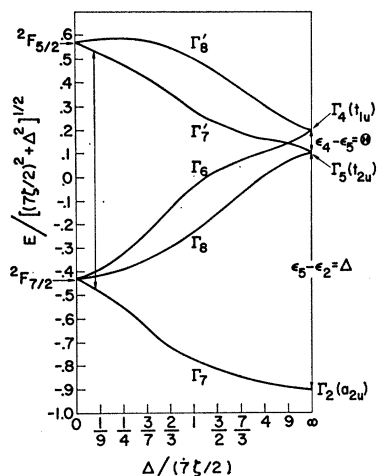


FIG. 1. The energy levels of f^{13} (one hole) as a function of the ratio of one of the cubic-crystal-field parameters, Δ , divided by the spin-orbit coupling parameter $(7\zeta/2)$. The vertical arrow near the left is the approximate situation for SrF_2 ($7\zeta/2 \gg \Delta$) and the observed $\Gamma_7' \rightarrow \Gamma_7$ transition. ($\Delta/\theta = 10$ was chosen to give agreement with the observed splitting. The details of the diagram are discussed subsequently in the text.)

of the host matrix. A very simple elastic-continuum model of the local compressibility is discussed in this connection and its use modifies this discrepancy slightly.

We felt it would be interesting to estimate the effect of covalent bonding upon the strain dependence with the hope that it might shed light upon some of the above difficulties. The rare-earth covalency calculations themselves have proved of interest since a reasonable fraction of the crystal-field splittings can be explained. In particular we calculate the contribution of σ and π bonding of the $4f$ electrons of Tm^{2+} in CaF_2 , etc. to the rare-earth energy-level splitting as well as the radial strain dependence of the splitting, transferred hyperfine structure (hfs), and orbital reduction factor. The very simple covalent model that we use is essentially that of Wolfsberg-Helmholz,¹⁷ adjusted to give good results for the transition metal ions ($3d^n$). Hartree-Fock rare earth and F^{-1} wave functions are used to calculate the overlap integrals. Briefly it is found that in addition to explaining a reasonably large fraction of the energy level splitting the radial dependence of the covalent contribution is slightly greater than predicted by an electrostatic model, and is thus in closer agreement with observation. The calculated amplitudes of the $4f$ orbitals at the F^{-1} nucleus are also of reasonable magnitude to explain the transferred hfs, but uncertainties as to the sign of the measured quantities and the importance of polarization effects makes the significance of this result uncertain. The orbital reduction, though experimentally quite small, is still an order of magnitude

¹⁷ See, for example, C. J. Ballhausen and H. Gray, *Molecular Orbital Theory* (W. A. Benjamin, Inc., New York, 1964), or C. J. Ballhausen, *Ligand Field Theory* (McGraw-Hill Book Company, Inc., New York, 1962).

larger than can be reasonably accounted for by covalency effects with this model. The importance of covalent bonding which these simple calculations suggest should serve to indicate the desirability of more careful and rigorous treatments in the future.

EXPERIMENTAL RESULTS AND IONIC MODEL

The crystal samples studied were doped with 0.1% and less Tm^{3+} and obtained from Optovac Corp. After being suitably oriented and shaped they were x-irradiated (50 keV, 16 h) to obtain the desired degree of conversion to Tm^{2+} . The load bearing faces were polished and gasketed with gold foil to insure even loading. The pressure was transmitted to the crystal mounted in the vacuum space of an optical cryostat from the ram of a piston driven by compressed gas mounted above the Dewar. The load was computed by a knowledge of the cross section of the crystal and the variable gas pressure in the piston. The fluorescence was excited by radiation from 100-W high-pressure Hg lamp filtered through a CuSO_4 solution. The sample temperature was about 8°K with liquid helium in the cryostat. A 1-m Ebert monochromator equipped with a 7500-line/in. Harrison grating was used in conjunction with a cooled PbS detector and lock-in amplification. Linewidths on the order of 0.1 cm^{-1} were observed with no applied stress. Some additional broadening due to inhomogeneous loading was sometimes observed. Measurements were made with applied stress along (100), (110), and (111) axes.

Figure 1 shows the energy level diagram for Tm^{2+} ($4f^{13}$) cubically coordinated with eight negative ions in $O_h(m\bar{3}m)$ symmetry. The figure displays the levels for the full ranges of the magnitudes of the spin-orbit coupling (ζ) to cubic field (V_c). The details of the diagram will be discussed in the next section. For the present purposes it will suffice to say that normally the rare earths are in the regime $\zeta \gg V_c$. The approximate position of the energy levels is shown on the figure by a vertical arrow representing the $\Gamma_7' \leftrightarrow \Gamma_7$ transition. In fluorescence the emission due to this transition occurs at¹⁴ $E(\Gamma_7' - \Gamma_7) = 8966.2 \text{ cm}^{-1}$ and is very intense.

We have measured the shift of the $E(\Gamma_7' - \Gamma_7)$ transition with uniaxial stress for three different orientations. Figure 2 shows that the results are independent of direction of applied stress as well as linear with applied stress. The result for $\text{Tm}^{2+} : \text{SrF}_2$ is $1.78 \times 10^{-10} \text{ cm}^{-1} (\text{dyn/cm}^2)^{-1}$ which is very close to our previously measured value¹⁶ of $1.75 \times 10^{-10} \text{ cm}^{-1} (\text{dyn/cm}^2)^{-1}$ for Tm^{2+} in CaF_2 .

Elementary group theoretical considerations show that for $\Gamma_7' \leftrightarrow \Gamma_7$ transitions the shift should be independent of the direction of applied stress. For the O_h group a general strain, ϵ , that transforms as the $a_{1g} + e_g + t_{2g}$ irreducible representations can be applied. However, since the antisymmetric direct product $\{\Gamma_7 \times \Gamma_7\} = a_{1g}$, the strains of the form $\epsilon(E)$ and $\epsilon(T_2)$

are ineffective on the Γ_7 levels.¹⁸ Thus, the only nonzero matrix element is $\langle \Gamma_7 | \epsilon(a_{1g}) | \Gamma_7 \rangle$. $\epsilon(a_{1g})$ is just the hydrostatic component of the strain. Writing $\epsilon(a_{1g})$ alternatively in terms of the fractional change in volume ($\Delta V/V \equiv \beta$) and elastic constants and bulk modulus (K)

$$\beta = \Delta V/V = \epsilon(a_{1g}) = (s_{11} + 2s_{12})p = p/3K,$$

where p is the applied stress. Using the known elastic constants for SrF_2 and assuming for the present that the local stress-strain relationship around a Tm^{2+} impurity is the same as for the bulk crystal, the experimental shift per unit strain is $dE(\Gamma_7' - \Gamma_7)/\beta = -364 \text{ cm}^{-1}$ as compared to the experimental result obtained for $\text{Tm}^{2+}:\text{CaF}_2$ of -499 cm^{-1} .

It is straightforward to compare the above quoted experimental numbers to what is predicted by the ionic model. The cubic crystal field can be written in terms of cubic harmonic operators¹⁹

$$V_c = -\frac{b_4}{60}[O_4^0 + 5O_4^4] + \frac{b_6}{180}[O_6^0 - 21O_6^4]. \quad (1)$$

Using the optical data of Kiss¹⁴ for $\text{Tm}^{2+}:\text{CaF}_2$, Bleaney¹⁹ has determined $b_4 = 45.8 \text{ cm}^{-1}$ and $b_6 = 5.05 \text{ cm}^{-1}$. For an ionic model one expects $b_4 \propto R^{-5}$ and $b_6 \propto R^{-7}$, where R is the radial distance to the charge that produces the cubic crystal field. Then using $\beta = \Delta V/V = 3dR/R$ and $\partial b_4/\partial R = -5b_4/R$ and $\partial b_6/\partial R = -7b_6/R$

$$\frac{dE(\Gamma_7' - \Gamma_7)}{\beta} = -\frac{50}{21}b_4 - 28b_6 - \frac{(96/147)}{E(\Gamma_7' - \Gamma_7)} \times [250b_4^2 + 2520b_4b_6 + 2469b_6^2] \quad (2)$$

is obtained, $E(\Gamma_7' - \Gamma_7) = 8966.2 \text{ cm}^{-1}$. The last term, in square brackets, is due to second-order crystal-field contributions but amounts to $\approx 30\%$ of the total. The higher order contributions, not shown, are negligible.¹⁶ Also omitted from Eq. (2) is the contribution from the volume dependence of the spin-orbit coupling parameter, which is expected to be small.²⁰ Using the above quoted values of b_4 and b_6 for $\text{Tm}^{2+}:\text{CaF}_2$ the theoretical value from Eq. (2) is $dE(\Gamma_7' - \Gamma_7)/\beta = -377 \text{ cm}^{-1}$. This is smaller than the experimental value of -499 cm^{-1} . For $\text{Tm}^{2+}:\text{SrF}_2$ the values of b_4 and b_6 have not been published. However, a rough fit to the spectra has been obtained²¹ assuming the ratio b_4/b_6 for Tm^{2+} to be the same in SrF_2 as in CaF_2 . (This is what is

¹⁸ A. A. Kaplianskii, *Opt. i Spektroskopiya* **16**, 1031 (1964) [English transl.: *Opt. Spectry. (USSR)* **16**, 557 (1964)].

¹⁹ B. Bleaney, *Proc. Roy. Soc. (London)* **A277**, 289 (1964).

²⁰ For example, from Dy^{2+} in the three compounds CaF_2 , SrF_2 , and BaF_2 [Z. J. Kiss, *Phys. Rev.* **137**, A1749 (1965)] one would calculate $\sim 13 \text{ cm}^{-1}$ for this term.

²¹ Z. J. Kiss and H. A. Weakliem, Technical Report AFAL-TR-64-334, 1965, p. 33 (unpublished).

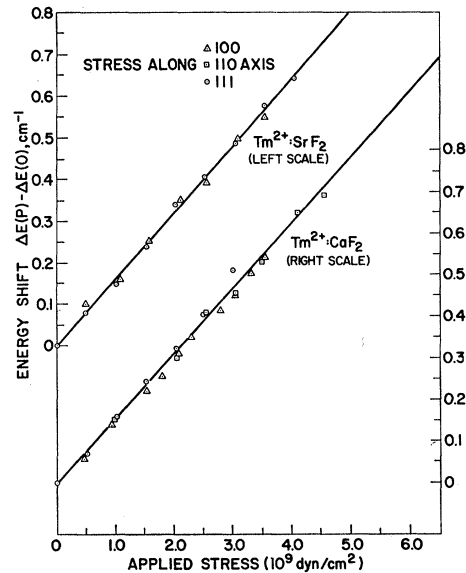


FIG. 2. The observed shift of Γ_7' to Γ_7 transition of Tm^{2+} versus applied stress along three directions for two different host lattices. Although the measured shift versus stress is very similar for the two hosts, due to a difference in elastic constants the shift per unit strain is about 35% smaller in SrF_2 .

found²⁰ for Dy^{2+} in the three hosts CaF_2 , SrF_2 , and BaF_2 .) Thus, for²⁰ $\text{Tm}^{2+}:\text{SrF}_2$ $b_4 = 38 \text{ cm}^{-1}$ and $b_6 = 38 (5.05/45.8) \text{ cm}^{-1}$ was used. The theoretical value from Eq. (2) is $dE(\Gamma_7' - \Gamma_7)/\beta = -295 \text{ cm}^{-1}$. This again is smaller than the experimental value of -365 cm^{-1} .

LOCAL COMPRESSIBILITY

Probably the greatest source of uncertainty in interpreting these pressure experiments arises from an uncertainty of the stress-strain relations which hold in the immediate vicinity of the defect being studied. Insight into the problem can be obtained from a study of the corresponding situation in a macroscopic elastic continuum. Such a model has been successful in discussing many of the properties of dilute alloys²² such as deviations from Vegard's law (additivity of lattice spacing of solid solutions).²³

Imagine placing an isotropic elastic "defect" sphere with an unconstrained radius R_D into a spherical hole with unconstrained radius R_M in an infinite isotropic elastic matrix. It is easiest to visualize the case $R_D > R_M$. Thus, the defect will be compressed to some equilibrium radius R . Then we apply an external pressure on the entire sample and ask how much the defect is compressed. The radial displacement of any point in the matrix, $u_M(r)$, or defect $u_D(r)$, for an arbitrary external

²² J. D. Eshelby, in *Solid State Physics*, edited by F. Seitz and D. Turnbull (Academic Press Inc., New York, 1956), Vol. 3, p. 79.

²³ J. Friedel, *Phil. Mag.* **46**, 514 (1955).

pressure (p_e) and internal pressure (p_i) is²⁴

$$|u_M(r) = -\frac{p_e}{3K_M}r + \frac{(p_i - p_e)R_M^3}{4\mu_M r^2}, \quad (3a)$$

$$u_D(r) = -\frac{p_i}{3K_D}r, \quad (3b)$$

where K_M (K_D) and μ_M are, respectively, the bulk and shear modulus of the matrix (defect). The internal pressure p_i is provided by the compression of the inner sphere

$$p_i = 3K_D(R_D - r)/R_D = 3K_D(\Delta R - u_M(R_M))/R_D, \quad (4)$$

where the equilibrium radius of the hole and sphere is $R = R_M + u_M(R_M)$ and $\Delta R = R_D - R_M$. The first term in Eq. (3a) is a compressive inward displacement whereas the second is a shear motion localized about the imperfection. Only compressive forces act on the defect as can be seen in Eq. (3b). By eliminating p_i from Eqs. (3a) and (3b) the equilibrium radius can be found for an arbitrary set of conditions. Finally we find for the displacements in the internal defect sphere

$$u_D(r) = p_e/3K_D^{\text{eff}}, \quad (5)$$

where

$$K_D^{\text{eff}} = (1 - \rho)K_D + \rho(R_D/R_M)K_M, \quad (6)$$

$$\rho = \frac{4}{3}\mu_M/(K_M + \frac{4}{3}\mu_M). \quad (7)$$

Equations (5)–(7) are the desired equations. They relate the strain of the elastic defect sphere to the external pressure via an effective bulk modulus K_D^{eff} . This effective bulk modulus depends on the equilibrium properties of both the host lattice and the defect lattice. Low-temperature ρ values of 0.374 and 0.387 are calculated from Eq. (7) for CaF_2 and SrF_2 , respectively.²⁴ In applying these results to nonisotropic solids an averaged sheard modulus $\langle\mu\rangle$ should be used²⁴

$$\langle\mu\rangle^{-1} = \left(\frac{2}{3}\right)(c_{44})^{-1} + \left(\frac{4}{3}\right)(c_{11} - c_{12})^{-1}. \quad (8)$$

The smallest defect unit which could reasonably be considered as having macroscopic elastic behavior is probably an (MF_8) cube, which is already so large that (R_D/R_M) differs from unity by only a few percent for either lattice. (We have used an estimate of 1.08 Å for the ionic radius of Tm^{2+} as compared to 1.00 Å for Ca^{2+} , 1.14 Å for Sr^{2+} .) The model thus predicts $K_D^{\text{eff}} \approx K_M + 0.6(K_D - K_M)$. We can only estimate a bulk modulus for TmF_2 because to our knowledge the pure material has never been prepared. In an ionic bonding model the bulk modulus scales inversely as the $\left(\frac{4}{3}\right)$ power of the atomic volume, other considerations being equal. This in turn predicts K_D^{eff} about midway between the

values²⁶ for CaF_2 and SrF_2 (0.95 and 0.75×10^{12} dyn/cm², respectively). K_D^{eff} for Tm^{2+} in CaF_2 is about 6% smaller than K_M and about 8% larger than K_M in SrF_2 . The influence of these corrections on the observed strain dependence will be considered subsequently. However, in view of the nature of the uncertainties involved, the above should probably best be considered as a semiquantitative estimate of the magnitude of the local compressibility correction. Microscopic calculations of the positions of the matrix atoms near an impurity atom have been performed²⁷ and used to interpret crystal fields. An extension of such a treatment to a consideration of the change of the fields with strain would be of interest.

COVALENT BONDING

By exploiting the well-known correspondence between a single electron and a single hole, it is possible to evaluate the elements of the Hamiltonian matrix $\mathfrak{H}' = \zeta \mathbf{L} \cdot \mathbf{S} + V_c$ for the states of the f^{13} system in the strong field representation. This representation is much more convenient to adopt when discussing covalent bonding than the more familiar weak field representation ($\zeta \gg V_c$). Upon diagonalization, these matrices yield five eigenvalues²⁸

$$E(\Gamma_6) = \frac{7}{2}\zeta + (1/7)(4\theta + \Delta), \quad (9)$$

$$E(\Gamma_7) = (3/7)\theta + \frac{1}{2}\left[\frac{7}{2}\zeta - (5/7)\Delta \pm \left\{\left(\frac{7}{2}\zeta\right)^2 - \Delta\zeta + \Delta^2\right\}^{1/2}\right], \quad (10)$$

$$E(\Gamma_8) = (1/7)\Delta + \frac{1}{2}\left[\frac{7}{2}\zeta + (1/7)\theta \pm \left\{\left(\frac{7}{2}\zeta\right)^2 - 2\theta\zeta + \theta^2\right\}^{1/2}\right], \quad (11)$$

where $\theta = \epsilon_4 - \epsilon_5$ and $\Delta = \epsilon_5 - \epsilon_2$ are the orbital energy differences in the strong-cubic-field limit. These energy differences are, of course, not observable because spin-orbit interaction cannot be "turned off," but they serve as convenient parameters. In fact it is important to realize that these energy differences along with ζ completely describe the splittings and the more familiar b 's [Eq. (1)] need never be mentioned. [As a convenience we list the relations between the b 's of Eq. (1) and the e 's: $\epsilon_2 = -12b_4 - 48b_6$; $\epsilon_4 = 6b_4 - 20b_6$; $\epsilon_5 = -2b_4 + 36b_6$.] Figure 1 shows the resulting energy levels as a function of the ratio of the cubic-field parameter Δ to the spin-orbit parameter ζ . The vertical line at the left of the diagram shows the approximate position of the energy levels of Tm^{2+} in CaF_2 . The values which fit the observed energy levels of Tm^{2+} :

²⁶ For low temperature elastic constants for CdF_2 see D. R. Huffman and M. H. Norwood, Phys. Rev. **117**, 709 (1960); for SrF_2 see D. Gerlich, *ibid.* **136**, A1366 (1964).

²⁷ For example see T. P. Das, Phys. Rev. **140**, A1957 (1965) and some of the references quoted there.

²⁸ J. C. Eisenstein and M. H. L. Pryce, Proc. Roy. Soc. (London) **A255**, 181 (1960); J. D. Axe, thesis [Lawrence Radiation Laboratory Report No. UCRL-9293, 1960 (unpublished)]. Available as Document No. 8127 from the Photoduplication Service, ADI Auxiliary Publications Project, Library of Congress, Washington 25, D. C. (unpublished).

²⁴ F. D. Murnaghan, *Finite Deformation of an Elastic Solid* (John Wiley & Sons, Inc., New York, 1951), p. 119.

²⁵ H. Brooks, *Impurities and Imperfections* (American Society for Metals, Cleveland, Ohio, 1955), pp. 22–23.

TABLE I. Linear combinations of ligand orbitals in cubic MX_8 complexes which can bond with f orbitals on the central ion. σ_i is a sigma orbital (along the internuclear distance) centered on the X ion and η_i and ξ_i are pi orbitals (perpendicular to the internuclear distance). As can be seen $4f$ orbitals that transform as the a_{2u} representation can form sigma but not pi bonds with the ligands, etc. The coefficients relating the group overlaps and the ion pair overlaps as calculated in the Appendix are given in the last column and are the same for $2s$ and $2p\sigma$ overlap integrals. The positions of atoms F referred to the nucleus M at the center of the cube, as origin, are (1) $(a/\sqrt{3})(1,1,1)$ (2) $(a/\sqrt{3})(\bar{1},1,\bar{1})$ (3) $(a/\sqrt{3})(1,\bar{1},\bar{1})$ (4) $(a/\sqrt{3})(\bar{1},\bar{1},1)$, where a is the length of the cube edge. The Miller indices for the vectors to describe the ligand $2p$ orbitals are

$\sigma_1(\bar{1},\bar{1},\bar{1})$	$\xi_1(1,\bar{2},1)$	$\eta_1(1,0,\bar{1})$
$\sigma_2(1,\bar{1},1)$	$\xi_2(\bar{1},\bar{2},\bar{1})$	$\eta_2(\bar{1},0,1)$
$\sigma_3(1,1,1)$	$\xi_3(1,2,\bar{1})$	$\eta_3(1,0,1)$
$\sigma_4(1,1,\bar{1})$	$\xi_4(\bar{1},2,1)$	$\eta_4(\bar{1},0,\bar{1})$

The positions and associated vectors for atoms (5), (6), (7) and (8) are obtained from those for (1), (2), (3), and (4) by inversion.

Representation (bond type)	Designation	Central ion orbital	Ligand orbitals	Group overlap ($S_{M\nu}$)
$a_{2u}(s \text{ and } p\sigma)$	$ \beta\rangle$	$(105)^{1/2}xyz$	$(8)^{-1/2}[\sigma_1+\sigma_2+\sigma_3+\sigma_4-\sigma_5-\sigma_6-\sigma_7-\sigma_8]$	$(40/9)^{1/2}\langle p\sigma f \rangle$
$t_{2u}(\pi)$	$ \epsilon_1\rangle$	$\frac{1}{2}(105)^{1/2}x(x^2-y^2)$	$(32)^{-1/2}[(\eta_2+\eta_3+\eta_5+\eta_8-\eta_1-\eta_4-\eta_6-\eta_7)+\sqrt{3}(\xi_1+\xi_3+\xi_6+\xi_8-\xi_2-\xi_4-\xi_5-\xi_7)]$	
	$ \epsilon_2\rangle$	$\frac{1}{2}(105)^{1/2}x(y^2-z^2)$	$(32)^{-1/2}[(\eta_2+\eta_4+\eta_5+\eta_7-\eta_1-\eta_3-\eta_6-\eta_8)+\sqrt{3}(\xi_1+\xi_3+\xi_6+\xi_8-\xi_2-\xi_4-\xi_5-\xi_7)]$	$(40/9)^{1/2}\langle p\pi f \rangle$
$t_{1u}(s \text{ and } p\sigma)$	$ \epsilon_3\rangle$	$\frac{1}{2}(105)^{1/2}y(z^2-x^2)$	$(8)^{-1/2}(\eta_1+\eta_2+\eta_7+\eta_8-\eta_3-\eta_4-\eta_5-\eta_6)$	
	$ \delta_1\rangle$	$\frac{1}{2}(7)^{1/2}z(5z^2-3r^2)$	$(8)^{-1/2}(\sigma_1+\sigma_4+\sigma_6+\sigma_7-\sigma_2-\sigma_3-\sigma_5-\sigma_8)$	
	$ \delta_2\rangle$	$\frac{1}{2}(7)^{1/2}x(5x^2-3r^2)$	$(8)^{-1/2}(\sigma_1+\sigma_3+\sigma_6+\sigma_8-\sigma_5-\sigma_7-\sigma_2-\sigma_4)$	$-(32/27)^{1/2}\langle p\sigma f \rangle$
$t_{1u}(\pi)$	$ \delta_3\rangle$	$\frac{1}{2}(7)^{1/2}y(5y^2-3r^2)$	$(8)^{-1/2}(\sigma_1+\sigma_2+\sigma_7+\sigma_8-\sigma_3-\sigma_4-\sigma_5-\sigma_6)$	
	$ \delta_1\rangle$	$\frac{1}{2}(7)^{1/2}z(5z^2-3r^2)$	$(32)^{-1/2}[(\xi_2+\xi_3+\xi_5+\xi_8-\xi_1-\xi_4-\xi_6-\xi_7)+\sqrt{3}(\eta_1+\eta_4+\eta_6+\eta_7-\eta_2-\eta_3-\eta_5-\eta_8)]$	
	$ \delta_2\rangle$	$\frac{1}{2}(7)^{1/2}x(5x^2-3r^2)$	$(32)^{-1/2}[(\xi_2+\xi_4+\xi_5+\xi_7-\xi_1-\xi_3-\xi_6-\xi_8)+\sqrt{3}(\eta_2+\eta_4+\eta_5+\eta_7-\eta_1-\eta_3-\eta_6-\eta_8)]$	$(1/2)^{1/2}\langle p\pi f \rangle$
	$ \delta_3\rangle$	$\frac{1}{2}(7)^{1/2}y(5y^2-3r^2)$	$(8)^{-1/2}(\xi_1+\xi_2+\xi_7+\xi_8-\xi_3-\xi_4-\xi_5-\xi_6)$	

CaF_2 are $\zeta = -2513 \text{ cm}^{-1}$, $\epsilon_2 = -792.0 \text{ cm}^{-1}$, $\epsilon_4 = 173.8 \text{ cm}^{-1}$, $\epsilon_5 = 90.2 \text{ cm}^{-1}$. We emphasize again that this procedure is thus far entirely consistent with the normal electrostatic field treatment but is more general in that the precise nature of the crystal-field interaction is not specified at the outset. The reason that the strong-field representation is convenient for the present purpose is that the quantities calculated by molecular orbital treatment, the ϵ_i 's appear in the energy expressions in place of the crystal-field parameters.

A set of ligand orbitals interact with only those metal orbitals which transform according to the same representation (Γ_i). A suitable set of irreducible ligand basis functions $\chi(\Gamma_i)$ and their metal-ion counterparts $\phi_M(\Gamma_i)$ are listed in Table I.⁸ While we have included $2p\sigma$, $2s$, and $2p\pi$ ligands in our basis set, we have not explicitly considered the effect of higher lying (e.g., $6s$, $6p$, $5d$) metal orbitals. Likewise we have not considered the effect of overlap of the ligands with themselves. We do not believe the inclusion of such effects will greatly modify our conclusions concerning the behavior of the $4f$ electrons. The secular equation, which follows from the variational treatment of the system, is of course factorable according to symmetry. Each of these systems of equations is of the form $|H_{ij} - S_{ij}E| = 0$ where H is the appropriate Hamiltonian operator for the

system and S_{ij} ($i \neq j$) are the group overlap integrals, i.e., the projections of the irreducible metal and ligand basis functions upon one another. Since these group overlaps are small it is permissible to obtain a perturbation solution to second order for E_i by replacing the off-diagonal terms $S_{ij}E$ by $S_{ij}H_{ij}$. For the bonding (B) and antibonding (A) states the wave functions are²⁹

$$\Psi^B(\Gamma_i, \nu) = \chi(\Gamma_i, \nu) + \gamma(\Gamma_i, \nu)\phi_M(\Gamma_i), \quad (12)$$

$$\Psi^A(\Gamma_i) = \phi_M(\Gamma_i) - \sum_{\nu} \lambda(\Gamma_i, \nu)\chi(\Gamma_i, \nu), \quad (13a)$$

$$\chi(\Gamma_i, \nu) = \sum_L a_L(\Gamma_i)\phi_L(\nu). \quad (13b)$$

The index ν refers to the three types of bonds s , $p\sigma$, and $p\pi$. Of course, the allowed values of ν for each irreducible representation are determined by symmetry (see Table I). The parameters that must be calculated are the $\lambda(\Gamma_i, \nu)$'s. [Note: By orthogonality of the bonding and antibonding wave functions $\lambda(\Gamma_i, \nu) = \gamma(\Gamma_i, \nu) + S_{M\nu}(\Gamma_i)$.] Solving the factored secular determinant for the antibonding energies E^A , with the above ap-

²⁹ The notation follows that of P. W. Anderson, in *Solid State Physics*, edited by F. Seitz and D. Turnbull (Academic Press Inc., New York, 1963), Vol. 14, p. 190ff where this type of calculation is briefly reviewed.

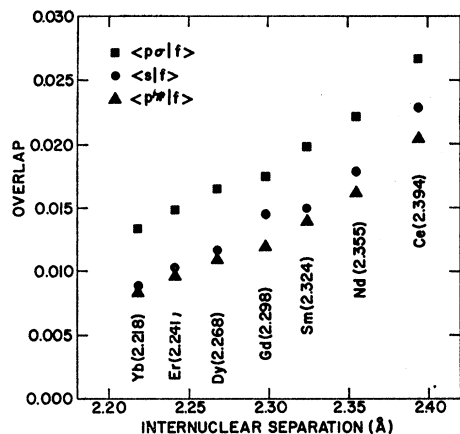


FIG. 3. Overlap for a number of (R.E.)³⁺-F³⁻ systems. This is the ion-pair overlap, e.g., $\langle 2p\sigma|4f \rangle$, etc., as in the Appendix, and not the group overlap $S_{M\nu}$. A plot of overlap at the equilibrium distance versus number of electrons would appear quite similar. Such a plot would display the fact that Eu⁺² and Gd⁺³ have very similar overlap (but of course at different equilibrium distances).

proximation for the off-diagonal values of E , we obtain

$$\epsilon_i \equiv E^A(\Gamma_i) = H_{MM}(\Gamma_i) + \sum_{\nu} \lambda^2(\Gamma_i, \nu) \times [H_{MM}(\Gamma_i) - H_{\nu\nu}(\Gamma_i)], \quad (14)$$

$$\lambda(\Gamma_i, \nu) = \left[\frac{H_{M\nu} - S_{M\nu}H_{MM}}{H_{\nu\nu} - H_{MM}} \right]_{\Gamma_i}. \quad (15)$$

[Note: In Eq. (15) we have started to suppress the index Γ_i and will continue to do this.] These two equations (14)–(15) completely describe the splittings of the three $4f$ levels provided the overlap $S_{M\nu}$ and the diagonal and off-diagonal matrix elements are known. $S_{M\nu}$ can be calculated in a straightforward manner provided the wave functions of the ions and internuclear distance are known. However, values for $H_{M\nu}$ are more troublesome.

In order to proceed further we make use of the Wolfsberg-Helmholz (W-H) approximation,¹⁷ by which the off-diagonal matrix elements $H_{M\nu}$ are assumed to have asymptotic values proportional to the overlap $S_{M\nu}$ and more particularly

$$H_{M\nu} = g \left(\frac{H_{MM} + H_{\nu\nu}}{2} \right) S_{M\nu}. \quad (16)$$

In conformity to much recent molecular-orbital (M. O.) treatments of transition metals¹⁷ we have chosen $g=2.0$ for both σ - and π -type interactions. The problem of estimating the covalency thus divides itself into two distinct parts. The first, calculating the overlap integrals presents no formal problem if a suitable set of wave functions exists. The second part of the problem is to find values for the diagonal matrix elements H_{kk} .

To calculate the overlap we have used analytical Hartree-Fock solutions expressed as sums of terms of the

simple Slater type. Therefore, the overlap integrals were readily evaluated by a transformation to spheroidal coordinates.^{17,30} Some details of these calculations are found in the Appendix. In order to gain some feeling as to the magnitude of overlap of $4f$ wave functions with $p\sigma$, $p\pi$, and s ligand orbitals and how these quantities vary within the rare-earth series sequence, Fig. 3 shows some results for a single fluoride ion-trivalent R. E. overlap at distances appropriate to the sum of their respective radii.³¹ As can be seen the various overlaps decrease by about 2 or 2½ when the $4f$ shell is filled. Quantitatively it appears that the shrinking of the internuclear distance (lanthanide contraction) with increasing atomic number fails to compensate for the decreasing radial extent of the $4f$ orbitals themselves.

The estimate more closely the possible covalent contributions to Eq. (14) in cubically coordinated (MX_8) divalent rare earths, wave functions³² and interatomic distances³³ appropriate to EuF₂ (2.592 Å) were used. The results for values of $S_{M\nu}$ are given in Table II. It can be argued using the results of Fig. 3. that the correction necessary for any other rare earth is no greater than two.

The remaining task of choosing appropriate values for the diagonal matrix elements H_{jj} is by no means as certain. Quite properly in an empirical treatment of this sort, the concern is not a detailed consideration of the

TABLE II. Summary of the contributions to the molecular-orbital calculation. The energy parameters used to calculate S and λ are $H_{MM} = -70 \times 10^3$ cm⁻¹, $H_{pp} - H_{MM} = -100 \times 10^3$ cm⁻¹, and $H_{ss} - H_{pp} = -200 \times 10^3$ cm⁻¹. On the right the logarithmic derivatives of S^2 is given. Thus, if $S \propto R^{-m}$ values for $2m$ are listed. The bottom of the table lists the various contributions to the energy of the three strong-field levels. These values are computed using Eqs. (14) or (17) as was done in Fig. 4. Note that the energies given here are one electron orbital energies, whereas Fig. 4 is an energy level diagram for a single hole in the $4f^{13}$ configuration for which the energies are inverted.

		a_{2u}	Orbital type t_{1u}	t_{2u}	$2m = 2 \left(\frac{R}{S} \right) \frac{dS}{dR}$
2s	S	0.0234	-0.0120	0.0	12.1
	λ	0.0288	-0.0148	0.0	
2pσ	S	0.0364	-0.0188	0.0	6.5
	λ	0.0619	-0.0319	0.0	
2pπ	S	0.0	0.0077	0.0231	10.4
	λ	0.0	0.0131	0.0393	
$\Delta = \lambda^2(H_{MM} - H_{\nu\nu})$		$\Delta(a_{2u})$	$\Delta(t_{1u})$	$\Delta(t_{2u})$	
	2s	249 cm ⁻¹	67 cm ⁻¹	0.0	
	2pσ	383	102	0.0	
	2pπ	0	17	154	
	Total	632	186	154	

³⁰ R. S. Mulliken, C. A. Reike, D. Orloff, and H. Orloff, J. Chem. Phys. **17**, 1248 (1949).

³¹ D. H. Templeton and C. H. Dauben, J. Am. Chem. Soc. **76**, 5237 (1954).

³² A. J. Freeman and R. E. Watson, Phys. Rev. **127**, 2058 (1962).

³³ T. R. McGuire and M. W. Shafer, J. Appl. Phys. **35**, 984 (1964).

nature of the terms in the Hamiltonian operator. Rather the concern is to find a set of numbers representing some "effective" Hamiltonian which when used in Eqs. (13)–(15) represent as closely as possible the true physical situation. This is the philosophy behind the extensive use¹⁷ of the Wolfsberg-Helmholz approximation in the M. O. calculations that are used to determine the energy splittings, etc. We have applied the Eqs. (13)–(15) to known values of 10 Dq and orbital-mixing parameters for several transition-metal complexes (e.g., NiF₆⁴⁻, etc.). Quite good agreement for NiF₆⁴⁻ 10 Dq and transfer hfs can be obtained using $H_{MM} = -120 \times 10^3$ cm⁻¹, $H_{pp} = -170 \times 10^3$ cm⁻¹, $H_{ss} = -370 \times 10^3$ cm⁻¹. For VF₆⁴⁻, 10 Dq was fitted with $H_{MM} = -75 \times 10^3$ cm⁻¹, $H_{pp} = -155 \times 10^3$ cm⁻¹, and $H_{ss} = -355 \times 10^3$ cm⁻¹. The numbers were chosen so that $H_{MM} - H_{pp}$ agree with experimental charge transfer energies (i.e., 50×10^3 cm⁻¹ for Ni-F and 80×10^3 cm⁻¹ for V-F).³⁴ In both cases the F^{-1} energies quoted above were approximately the same. For the rare earths the value of the quantity $H_{MM} - H_{pp}$ should also coincide with charge-transfer excitations of the complex, and while we know of no direct measurements for divalent rare earths an estimate of $H_{MM} - H_{pp} \approx 100 \times 10^3$ cm⁻¹ seems reasonable, based upon what is known for trivalent rare earths and the general systematics of charge-transfer excitation.³⁴ In the absence of any strong physical arguments to the contrary, we would suppose that the matrix elements H_{pp} and H_{ss} for the fluoride ligands will not differ appreciably in rare earths as opposed to transition metal complexes. (It seems sensible that H_{MM} is less negative for rare-earth ions than transition metals because the 4f electrons are much less strongly bound in the free ion.) Thus, taking the above values of H_{pp} and H_{ss} as central values we have evaluated covalent energy contributions, but have chosen to introduce some variation more or less concomitant with our uncertainty in the parameters by fixing $H_{MM} - H_{pp} = 100 \times 10^3$ cm⁻¹, $H_{pp} - H_{ss} = 200 \times 10^3$ cm⁻¹, and by varying H_{MM} . The energy levels as a function of H_{MM} are shown in Fig. 4 and Table II lists a breakdown of the contributions to the energy for a particular set of parameter values quoted in the caption. We imagine that the more plausible values for the parameters lie near the center of Fig. 4. There are two points of interest to be made. First the magnitude of the predicted covalent³⁵ contribution to the splitting (≈ 480 cm⁻¹) is a rather substantial

³⁴ C. K. Jorgensen, *Absorption Spectra and Chemical Bonding in Complexes* (Pergamon Press, Ltd., Oxford, 1962). When treated consistently by M.O. theory, the energy denominator in Eq. (15) refers to virtual excitations of the complex, rather than an experimentally observable charge transfer energy as has been traditionally (and somewhat carelessly) used in semiempirical treatments. However, Sugano and Tanabe (Ref. 46) have recently shown this procedure to be justifiable on empirical grounds.

³⁵ We mean by covalent energy contributions all those terms which depend upon nonvanishing overlap with the ligands, which is traditional usage. According to a more specific usage in the recent physics literature (Ref. 42) our covalent energy is the sum of renormalization, overlap, and covalent contributions.

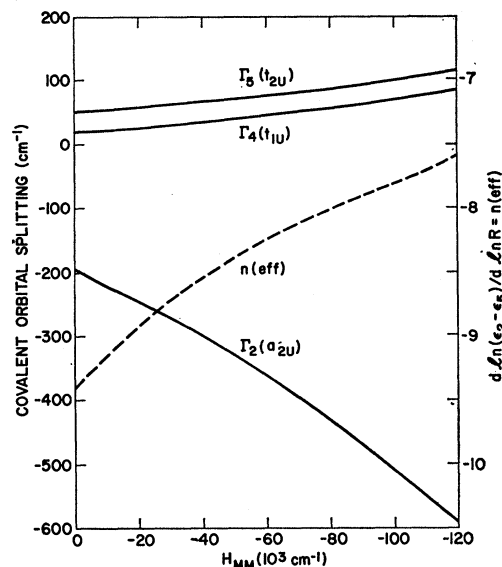


Fig. 4. A plot of the splitting resulting from overlap as a function of the diagonal metal matrix element H_{MM} . The splittings of the three strong-field energy levels are drawn so the center of gravity is unshifted. Although the maximum splitting varies from about 250 to 700 cm⁻¹ as H_{MM} becomes more negative, as discussed in the text, the most probable value is $\sim -70 \times 10^3$ cm⁻¹. For this value of H_{MM} the orbital splittings are given in Table II. The dashed line is a plot of n_{eff} versus H_{MM} . This quantity (≈ 8.2 at $H_{MM} = -70 \times 10^3$ cm⁻¹) can be used for comparison with the strain experiment and the electrostatic model.

portion of the total observed splitting (e.g., 960 cm⁻¹ for Tm²⁺:CaF₂). In this regard it should be mentioned that Bleaney¹⁹ has calculated the splitting to be expected due to a CaF₂ lattice of point charges and finds that it accounts for only about $\frac{1}{4}$ of the observed splitting. This is just one example of the general insufficiency of the point-charge model in calculating rare-earth splittings.¹⁻³ The second point of interest is that covalent interaction alone leaves the t_{1u} and t_{2u} levels very close together in agreement with what is observed experimentally. In any electrostatic model using the full interatomic distances the fourth-order term dominates the sixth-order term which places the t_{2u} level about midway between the t_{1u} and a_{1u} levels. Note from Table II that although $p\sigma$ bonding contributions dominate the over-all splitting pattern s overlap accounts for 39% of the a_{2u} energy while s and $p\pi$ overlaps account for 36% and 9%, respectively, of the t_{1u} covalent orbital energy.

STRAIN DEPENDENCE, HYPERFINE INTERACTION AND ORBITAL REDUCTION IN A COVALENT MODEL

The preceding section indicates that it would not be unreasonable to expect sizable covalent contributions to the 4f cubic-crystal-field splitting. Thus, it becomes immediately interesting to estimate some of the other consequences of this covalent contribution.

We can calculate the strain dependence of the covalent contribution using Eqs. (13)–(16). The covalent splitting is the sum of terms contributed by overlap with the ν th ligand set.

$$E^A(\Gamma_i) - H_{MM}(\Gamma_i) = \sum_{\nu} [[H_{\nu\nu}^2 / (H_{MM} - H_{\nu\nu})] S_{M\nu}^2]_{\Gamma_i}. \quad (17)$$

If the diagonal elements H_{jj} could be treated as a constant, the radial dependence would be determined by the behavior of $S_{M\nu}$. Even though the H_{jj} differ substantially from the free-ion values because of mutual interactions in the crystal, we can justify neglecting the radial dependence of $H_{\nu\nu}^2 / (H_{MM} - H_{\nu\nu})$ so long as $H_{MM} - H_{\nu\nu}$ is not very small compared with $H_{\nu\nu}$. This is because it is likely that the largest radially dependent fractions of the H_{jj} are Coulombic and have the relatively slow R^{-1} dependence.

It is convenient to specify the radial dependences of quantities by their logarithmic derivatives $[(R/f(R)) (df/dR)]_{R=R_{eq}}$. In particular the logarithmic derivative of the orbital splitting $(\epsilon_2 - \epsilon_5) = \Delta$ we shall call n_{eff} because at the equilibrium distance Δ and $d\Delta/dR$ are given correctly by an expression of the form (constant) $\times R^{n_{eff}}$. We need concern ourselves only with the behavior of Δ because from Eq. (10) the strain dependence of the observed transition $E(\Gamma_7' - \Gamma_7)$ depends only upon Δ . Each of the individual overlap contributions has a different radial dependence as seen in Table II, and the net contribution to n_{eff} varies as shown in Fig. 4, according to the relative magnitude of the s , $p\sigma$, and $p\pi$ contributions. By way of comparison, in the electrostatic model n_{eff} depends only upon the ratio (b_6/b_4) and from Eqs. (2) and (10) a value of -6.03 is predicted for both $Tm^{2+}:\text{CaF}_2$ and $Tm^{2+}:\text{SrF}_2$. The "observed" values of n_{eff} , that is the changes in Δ implied by the measured strain dependences of $E(\Gamma_7' - \Gamma_7)$, can be calculated with the aid of Eq. (10). They are -6.9 for $Tm^{2+}:\text{CaF}_2$ and -6.7 for $Tm^{2+}:\text{SrF}_2$ assuming that bulk compressibilities hold locally. If the compressibilities are corrected along the lines discussed in the section on local compressibility the values are -6.5 and -7.2 , respectively. Thus, while the radial dependence of the electrostatic model seems slightly too weak, that of a purely covalent model is slightly too strong. It is worth pointing out that π bonding in the t_{2u} levels decreases $\epsilon_2 - \epsilon_5$ and thus also n_{eff} . Incidentally we also find that the change in the square of the overlap accounts for the observed strain dependence of transition metal complexes in the instances³⁶ we have investigated.

Among the consequences of small amounts of covalency, one of the most readily observable is the change in magnetic moment due to "orbital reduction." We may write the two hole states comprising the lowest Kramer's doublet in Tm^{2+} in a cubic (MX_8) environ-

ment as²⁸

$$\begin{aligned} |\Gamma_7\rangle &= \cos\delta |A\rangle + \sin\delta |B\rangle, \\ |\Gamma_7^*\rangle &= \cos\delta |\bar{A}\rangle + \sin\delta |\bar{B}\rangle, \end{aligned} \quad (18)$$

where

$$\begin{aligned} |A\rangle &= i|\beta\rangle; |B\rangle = (3)^{-1/2} [|\epsilon_1^+\rangle + |\epsilon_2\rangle + i|\epsilon_3\rangle], \\ |\bar{A}\rangle &= i|\bar{\beta}\rangle; |\bar{B}\rangle = (3)^{-1/2} [-|\bar{\epsilon}_1\rangle + |\epsilon_2^+\rangle - i|\epsilon_3^+\rangle]. \end{aligned} \quad (19)$$

Here $|\beta^+\rangle$, etc., are products of orbital wave functions given in Table I and the $|\pm\rangle$ spin eigenfunctions. $|A\rangle$, $|B\rangle$ and $|\bar{A}\rangle$, $|\bar{B}\rangle$ form bases for the Γ_7 representation. The proper value of δ is obtained by diagonalization of $3C'$ and is given by

$$\tan\delta = (2\sqrt{3})^{-1} \cdot \{(\Delta - \frac{1}{2}\zeta) - [(\frac{7}{2}\zeta)^2 - \Delta\zeta + \Delta^2]^{1/2}\}. \quad (20)$$

Orbital reduction can be specified phenomenologically by two parameters

$$\begin{aligned} k &= \langle A | L_Z | B \rangle / \langle f_A | L_Z | f_B \rangle, \\ k' &= \langle B | L_Z | B \rangle / \langle f_B | L_Z | f_B \rangle, \end{aligned} \quad (21)$$

where $(|f_A\rangle, |f_B\rangle)$ represents $(|A\rangle, |B\rangle)$ in the limit of no ligand admixing. (A third reduction factor involving $\langle A | L_Z | A \rangle$ proves unnecessary because $\langle A | L_Z | A \rangle = \langle f_A | L_Z | f_A \rangle = 0$.) The g factor for this lowest Kramer's doublet is given by

$$\begin{aligned} g(\Gamma_7) &= 2\langle \Gamma_7 | L_Z + g_s S_Z | \Gamma_7 \rangle \\ &= g_s \cos^2\theta + (8/\sqrt{3})k \cos\theta \sin\theta \\ &\quad + (\frac{1}{3})(2k' - g_s)\sin^2\theta. \end{aligned} \quad (22)$$

(This expression is more generally valid than that given by Bleaney,¹⁹ who assumed identical orbital reduction factors for all orbital states.) The orbital reduction factors introduced in Eqs. (21) and (22) can be evaluated in terms of the M.O. wave functions arrived at in the previous section by direct substitution. After a rather tedious calculation following Stevens,³⁷ we obtain to lowest order in λ^2

$$\begin{aligned} k &= 1 - [\lambda^2(a_{2u}, s) + \lambda^2(a_{2u}, p\sigma) + \sqrt{\frac{2}{3}}\lambda(a_{2u}, p\sigma) \\ &\quad \times \lambda(t_{2u}, p\pi) + \lambda^2(t_{2u}, p\pi)], \quad (23) \\ k' &= 1. \end{aligned}$$

For the range of values of H_{MM} represented in Fig. 4, the calculated values of $1 - k$ lie between 1.3×10^{-3} and 0.3×10^{-3} . The value of $1 - k$ necessary to explain the observed g value is $0.011 (\pm 0.001)$ which is larger by at least an order of magnitude. Put another way, using our estimates of the relations between ligand admixing and covalent energies, the orbital admixtures necessary to explain the observed discrepancy in the g value would result in covalent splitting terms about 5 times greater than the total observed splittings. These results seem therefore to lend credence to Inoue's suggestion³⁸ that mixing of electronic states due to multiple phonon

³⁷ K. W. H. Stevens, Proc. Roy. Soc. (London) **A219**, 542 (1953).

³⁸ M. Inoue, Phys. Rev. Letters **11**, 196 (1963). Also R. Orbach and P. Pincus, Phys. Rev. **143**, 168 (1966).

³⁶ G. Burns and J. D. Axe, J. Chem. Phys. (to be published).

processes contributes strongly to the small magnetic moment anomaly in $\text{Tm}^{2+}:\text{CaF}_2$.

One of the most valuable methods of investigating covalency in transition-metal fluoride complexes has been through the observation in the electron paramagnetic resonance of anomalous hyperfine interaction of the F^{19} nuclear spin with the nonlocalized electronic spin of the complex. Bessent and Hayes⁹ have studied this effect by ENDOR techniques in $\text{Tm}^{2+}:\text{CaF}_2$. For simplicity we consider only the contact term which is assumed to arise from admixtures of $2s$ orbitals of nearest fluorine ligands. The corresponding term in the spin Hamiltonian is $\sum_i A_i^s \mathbf{S} \cdot \mathbf{I}_i$ where the sum is over the eight nearest F^{1-} neighbors and a comparison of the matrix elements of this spin Hamiltonian with those using the wave functions given in Eq. (18) yields

$$A_i^s = [\cos^2 \delta] \lambda^2 (a_{2u,s}) A_{2s} / 8. \quad (24)$$

Here $A_{2s} = 45.0$ kMc/sec is the calculated hyperfine interaction constant evaluated for a $2s$ electron in F^{1-} . This leads to calculated values of A_i^s ranging from $+1.8$ Mc/sec to $+3.6$ Mc/sec, as compared to the measured value of ± 2.584 Mc/sec reported by Bessent and Hayes.⁹ Although the sign of the measured value is uncertain in Tm^{2+} , other processes (presumably involving polarization of outer filled rare-earth orbitals³⁹) cause A_i^s to be negative in Eu^{2+} .⁸ It is therefore not clear what significance is to be attached to the order of magnitude agreement noted above.

SUMMARY AND DISCUSSION

(1) There has been relatively little experimental work on stress effects in $4f \leftrightarrow 4f$ transitions,⁴⁰ although the symmetry aspects of uniaxial stress effects have received some attention.¹⁸ However, stress measurements contain valuable information concerning the radial dependence of crystal-field interactions, which can be checked for example, with the prediction of an electrostatic model.¹⁶

(2) It has been shown that for Tm^{2+} in both CaF_2 and SrF_2 the experimentally observed radial dependence is somewhat larger than predicted by the electrostatic model if the macroscopic stress-strain relation is assumed to hold at the position of the Tm^{2+} ion. The use of an elastic continuum model to estimate the "local" compressibility does not produce substantially better results.

(3) We have performed a semiempirical, Wolfsberg-Helmholz type, molecular-orbital calculation to determine the energy splittings of rare earths in cubic (O_h) symmetry in particular for MF_8^{-6} . The off-diagonal matrix elements are set equal to the product of the overlap times an average of the diagonal matrix elements. The diagonal matrix elements are varied

between some reasonable limits. This treatment predicts that a considerable fraction of the cubic crystal field can be explained as coming from overlap of the $4f$ electrons with the ligands. This is in general agreement with the conclusions of Jorgensen *et al.*¹⁰ A simple argument leading directly to this conclusion can be presented. The magnitude of the covalent antibonding energy shift is proportional to the square of the overlap with the neighboring ligands [see Eq. (17)]. Thus, in a rough way the total splitting of the levels is $\propto S^2$ where S is the largest overlap. The ratio of S^2 for iron group fluorides to that for R.E. fluorides is ≈ 10 , which is also roughly the ratio of $10 Dq$ to the strong-field orbital energy splittings for rare-earth fluorides. Since the splittings for the iron group are known to originate from covalent effects predominantly, we should not therefore be surprised to find sizeable covalent contributions in rare earths also.

A strong-ligand-field representation is used since it is the strong-field eigenvalues (the ϵ_i 's) that are directly calculated in the M.O. treatment. These one-electron orbital-energy differences $\Delta = \epsilon_5 - \epsilon_2$ and $\theta = \epsilon_4 - \epsilon_5$ together with ζ constitute a convenient and equally valid alternative set of parameters to the usual set of cubic-crystal-field parameters b_4 , b_6 , and ζ .

(4) The traditional electrostatic contribution to the energy splittings is of course still to be considered. Thus, using what we believe to be reasonable values for the diagonal matrix elements, Table II shows that $\sim 50\%$ of the energy splitting can be accounted for by covalency. However, the familiar electrostatic crystal-field terms occur in the Hamiltonian as well, and in general increase the magnitude of the splitting. What is not obvious and will take a more careful treatment to untangle is to what extent these electrostatic effects have been inadvertently mixed with covalency by our empirical method of parameter selection.⁴¹ Nevertheless, the fact that in an M.O. treatment for rare earths, less crystal field is required to come from electrostatic effects is in right direction since, in general, electrostatic calculations of the fields due to the surrounding ions are smaller than the experimentally observed fields.¹⁻³ However, there are still uncertainties as to the detailed values to be obtained from the electrostatic model associated with, for example, the detailed distribution of charge.⁷

(5) It should also be emphasized that there exist several first principle calculations of overlap effects for the iron series ions.⁴²⁻⁴⁶ These calculations determine the

⁴¹ M. H. Cohen, and V. Heine, *Phys. Rev.* **122**, 1821 (1961).

⁴² R. G. Schulman and S. Sugano, *Phys. Rev.* **130**, 506 (1962); K. Knox, R. G. Shulman, and S. Sugano, *ibid.* **130**, 512 (1962); S. Sugano and R. G. Shulman, *ibid.* **130**, 517 (1962).

⁴³ R. E. Watson and A. J. Freeman, *Phys. Rev.* **134**, A1526 (1964).

⁴⁴ E. Simanek and Z. Sroubek, *Phys. Status Solidi* **4**, 251 (1964).

⁴⁵ J. Hubbard, D. E. Rimmer, and F. R. A. Hopgood, *Proc. Phys. Soc.* **88**, 13 (1966).

⁴⁶ S. Sugano and Y. Tanabe, *J. Phys. Soc. Japan* **20**, 1155 (1965).

³⁹ R. E. Watson and A. J. Freeman, *Phys. Rev. Letters* **6**, 277 (1961).

⁴⁰ A. A. Kaplianskii and A. K. Przhnevskii, *Opt. Spektroskopiya* **13**, 882 (1962) [English transl.: *Opt. Spectry. (USSR)* **13**, 508 (1962)]; and Z. J. Kiss (unpublished).

amount of ligand admixing by directly solving the wave equation. Thus, the values for the matrix elements H_{ij} are directly calculated (rather than estimated as is done when using the Wolfsberg-Helmholz method). The empirical treatment we have attempted is not an adequate substitute for a more detailed analysis, and such a calculation would be most welcome. The present treatment does however have the advantage of being simple and lucid. Also the semiempirical methods used here usually produce good results¹⁷ in transition metals.

(6) We have also used this model to estimate some of the consequences of what we believe to be a non-negligible covalent bonding contribution.

The covalent contribution to the cubic-crystal-field parameter Δ is proportional to $\sim R^{-8}$, whereas the electrostatic contribution is $\sim R^{-6}$, and the experimental results are about midway between. The result is consistent with a large but not dominant covalent contribution.

We have calculated the orbital reduction factor (the deviation of the g value of the lowest state caused by ligand orbital admixtures). We are unable to explain the magnitude of this factor even though it is not large. This result lends credence to the suggestion³⁸ that phonon admixing of electronic states contribute to the small deviations from the expected g values for $\text{Tm}^{2+}:\text{CaF}_2$.

Finally, we have calculated the contact term in the transferred hyperfine Hamiltonian of $(\text{TmF}_3)^{6-}$. The magnitude of the result is in agreement with experiment. However, the sign of the experimental result is uncertain, and the issue is further clouded by the possibility of large core polarization effects.³⁹ In addition, it

has recently been shown⁴²⁻⁴⁶ that a somewhat different effective Hamiltonian should be used to calculate unpaired ligand spin density than that used for calculation of the energies of the antibonding states.

ACKNOWLEDGMENTS

It is a pleasure to thank B. A. Jenkins for capable experimental help, J. E. Scardefield for the initial crystal used, and Dr. A. S. Nowick for a discussion on the local-compressibility problem.

APPENDIX

The analytical radial wave functions for the fluoride ion were those used by Sugano and Shulman⁴²

$$\chi_{2p} = 15.671\phi_{2p}(3.7374) + 1.5742\phi_{2p}(1.3584), \quad (\text{A1})$$

$$\chi_{2s} = -11.156\phi_{1s}(8.70) + 10.805\phi_{2s}(2.425), \quad (\text{A2})$$

whereas the rare-earth functions as determined by Freeman and Watson³² are all of the type

$$\chi_{4f} = \sum_{i=1}^4 N_i \phi_{4f}(\mu_i), \quad (\text{A3})$$

where $\phi_{nl}(\mu) = (r^{n-1}e^{-\mu r})Y_l^m(\theta, \phi)$. The overlap integrals between ion pairs can then be written as sums of overlap integrals of the simple Slater type $s(nl, n'l', R) = \langle \phi_{nl} | \phi_{n'l'} \rangle$, where R is the internuclear distance. Mulliken *et al.*^{30,17} have shown how to evaluate such expressions in terms of the incomplete gamma functions $A_k(p) = \int_1^\infty \xi^k e^{-p\xi} d\xi$, and $B_k(p) = \int_{-1}^1 \eta^k e^{-p\eta} d\eta$. Several overlap expressions involving $4f$ Slater functions are as follows:

$$\begin{aligned} \langle 1s | 4f \rangle &= (7/16)^{1/2} (R/2)^6 [(-5B_2 + 3B_4)A_0 + (9B_3 - 3B_5)A_1 \\ &\quad + (5B_0 - 9B_4)A_2 + (-9B_1 + 5B_5)A_3 + (-3B_0 + 9B_2)A_4 + (3B_1 - 5B_3)A_5], \\ \langle 2s | 4f \rangle &= (7/16)^{1/2} (R/2)^7 [(-5B_3 + 3B_5)A_0 + (-5B_2 + 12B_4 - 3B_6)A_1 + (5B_1 + 9B_3 - 12B_5)A_2 \\ &\quad + (5B_0 - 9B_2 - 9B_4 + 5B_6)A_3 + (-12B_1 + 9B_3 + 5B_5)A_4 + (-3B_0 + 12B_2 - 5B_4)A_5 + (3B_1 - 5B_3)A_6], \\ \langle 2p\sigma | 4f \rangle &= (21/16)^{1/2} (R/2)^7 [(-5B_2 + 3B_4)A_0 + (4B_3)A_1 + (5B_0 - 3B_6)A_2 \\ &\quad + (-4B_1 - 4B_5)A_3 + (-3B_0 + 5B_6)A_4 + (4B_3)A_5 + (3B_2 - 5B_4)A_6], \\ \langle 2p\pi | 4f \rangle &= (63/128)^{1/2} (R/2)^7 [(5B_2 - 6B_4 + B_6)A_0 - (8B_3 - 8B_5)A_1 + (-5B_0 + 11B_4 - 6B_6)A_2 - (-8B_1 + 8B_5)A_3 \\ &\quad + (6B_0 - 11B_2 + 5B_6)A_4 - (8B_1 - 8B_3)A_5 + (-B_0 + 6B_2 - 5B_4)A_6]. \end{aligned}$$

Note that these formulas are for use with unnormalized radial wave functions $\phi_{nl}(\mu)$ defined above.

The above overlap integrals for a pair of atoms must be related to the more complicated group overlap of a central ion with the appropriate set of symmetry adapted ligand functions in order to be useful. This can always be performed by a suitable set of coordinate transformations. The results for the group overlap involving the 8 cubic-basis ligand functions are included in Table I.

As previously explained, the radial dependence of covalent splittings has been characterized by a number

n_{eff} . This is convenient for comparison with multipole electrostatic splittings which are proportional to R^{-n} . This is not meant to imply that covalent splittings are well represented by $S = \text{const } R^{-m}$ over any appreciable range however. In fact, if S is to be extrapolated for large changes of R a better form is probably⁴⁷ $S = B \exp(-R/\rho)$. To go from one form to the other is quite trivial since $m = R_0/\rho$ where R_0 is the internuclear distance for which m is calculated. ρ is apparently independent of R over a reasonably large range of R .⁴⁷

⁴⁷ D. W. Hafemeister and W. H. Flygare, *J. Chem. Phys.* **43**, 795 (1965).